

Implementation of Phase-Shifting Transformer model into an OPF formulation by Matlab optimization toolbox

J. M. García-Guzmán*, F. J. Ortega-Herrera*, J. Torres-Jiménez**, G. Tapia-Tinoco**, L. A. Contreras-Aguilar**

* Department of Electromechanical Engineering, Instituto Tecnológico Superior de Irapuato

** Department of Postgraduate in Electrical Engineering, Instituto Tecnológico Superior de Irapuato

Abstract- This paper presents the practical implementation of Phase-Shifting Transformer (PST) model into an Optimal Power Flow (OPF) problem by using the Matlab optimization toolbox. The complexity degree related to the proposed implementation is equivalent to that required by commercial optimization packages for solving optimization models, but with the advantage that Matlab is commonly the available software for research and academic purposes in electric engineering. Thus, this hugely reduces the time to the implementation, and for obtaining results of an OPF analysis of power systems with embedded FACTS devices, in this case with the Phase-Shifting Transformer model. The reliability of the proposed implementation is proved by comparing the PST-OPF solution of the 5-node system with reported results in the open literature. In order to illustrate numerically the prowess of the proposed Matlab based implementation to solve the PST-OPF model, a numerical example with the 10-machine 39-bus New England test system is presented.

Index Terms- Electric power system, Matlab, OPF, optimization, PST

I. INTRODUCTION

The growth of electric power consumption in most countries is certain to continue unabated in the foreseeable future and the problems faced by the Electric Utilities in delivering the demanded power are increasing. The Phase-Shifting Transformer is one special application of transformers that will help utilities to better utilise existing transmission corridors and to improve on the operation of the system [1].

When power flows between two nodes, there is a voltage drop and a phase angle shift between the sending node and receiving node, which depend on the magnitude and angle of the load current. The Phase-Shifting Transformer compensates for the drop by inserting, between its sending and its receiving nodes, a series voltage in quadrature with the line-to-ground voltage. This quadrature voltage produces, between the PST terminals, a phase shift whose magnitude varies with the magnitude of the quadrature voltage, hence, the term phase-shifting transformer. The quadrature voltage is obtained from the shunt connected three phase transformer, called exciting transformer. It is inserted into the PST terminals via the series connected transformer, called the booster transformer [2].

Some significant benefits obtained by using the PST are: a) Reduction of active power losses by eliminating circulating

currents; b) Improvement in of transmission line capability through proper division of the power flow; c) Control of power flow [2].

With the worldwide increasing of the installation of FACTS devices in the electric power systems, OPF studies considering these devices are being used. An OPF analysis gives an answer to how the available controls should be adjusted in order to meet demand in the most economically manner while keeping within bounds all the constraints imposed on the system. Hence, the incorporation of the PST model into an OPF algorithm provides an opportunity to fully exploit the controller's capabilities in the economic operation of power systems.

In order to solve OPF models and, at the same time speed up the research of optimization applications, researchers have put attention on commercial optimization software packages as AMPL [3] and GAMS [4]. By way of example, AMPL and GAMS has been employed to: solve an OPF model with complementary constraints [5], identify and analyze saddle node bifurcations and limit-induced bifurcations of power systems [6], solve a transient stability constrained OPF model [7] and more recently to solve a OPF model that considers voltage stability constraints in order to control voltage stability of power systems [8] and to find the optimal location of FACTS shunt series controllers for power system operation planning [9], among other applications.

The Matlab optimization toolbox [10] was used in [11] to implement and solve a conventional OPF model. In this paper, such a proposal is adopted and extended to develop the implementation and solution of an OPF model integrated with PST model, here called PST-OPF model. In this sense, the complexity degree of the proposed implementation is equivalent to that required by commercial optimization packages for solving optimization models. Therefore, this proposal hugely reduces the time to the implementation and for obtaining results of an OPF analysis of power systems with PST device.

The paper's structure is as follows; Section II of the paper shows the general OPF formulation. The power system components and PST modelling are presented in the Section III. Section IV shows the explicit PST-OPF formulation. The computational implementation of the PST-OPF model is described in Section V. The prowess of the proposed implementation is illustrated by means of numerical examples in Section VI. The work conclusions are given in Section VII.

II. GENERAL OPF FORMULATION

The OPF general formulation is given in [11],

$$\text{Minimize } f(y) \quad (1)$$

$$\text{Subject to } h(y) = 0 \quad (2)$$

$$g(y) \leq 0 \quad (3)$$

$$y_{\min} \leq y \leq y_{\max} \quad (4)$$

where $f(y)$ is the objective function, $h(y)$ is a set of equality constraints representing both, power balance mismatch equations and control equations, $g(y)$ is a set of inequality constraints modelling the generator output reactive power limits. The vector of system variables y is bounded by lower and upper limits y_{\min} and y_{\max} , respectively. The solution vector of the model (1)-(4) yields the desired optimum point y^* .

III. POWER SYSTEM AND PST MODELLING

In order to assemble a full PST-OPF power system model, it is necessary to represent by means of a mathematical model the steady state operation of the power system components as well as the PST controller. In this work these models are described in polar coordinates, in terms of active and reactive power flow injections, as given below.

A. Power system main components

The generators, loads, shunt compensation elements, transmission lines and transformers are considered the most common power system components. The steady state power flow models of the above mentioned components are given in detail in [12] and are adopted in this proposal.

B. Phase-Shifting Transformer modelling

1) Phase-Shifting Transformer

The PST device is capable of redirecting power flows by locally altering the voltage angle difference imposed on the device by network conditions. When power flows between two nodes, there is a voltage drop and a phase angle shift between the sending node and receiving node, which depend on the magnitude and angle of the load current. Figure 1 shows a transmission line representation and its phase diagram, where it is assumed that the line current I_{ps} is in phase with the voltage magnitude V_p [2].

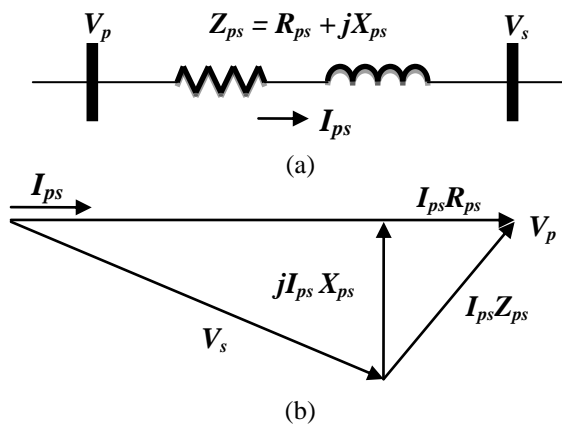


Figure 1: Transmission line representation.

Figure 1 (b) shows the voltage drop $jI_{ps}X_{ps}$ is in quadrature with the system line-to-ground voltage V_p . The PST compensates for the $jI_{ps}X_{ps}$ drop by inserting, between its sending and its receiving

nodes, a series voltage in quadrature with the line-to-ground voltage. This quadrature voltage produces, between the PST terminals, a phase shift whose magnitude varies with the magnitude of the quadrature voltage, hence, the term phase-shifting transformer. The quadrature voltage is obtained from the shunt connected three phase transformer, called exciting transformer. It is inserted into the PST terminals via the series connected transformer, called the booster transformer.

2) The classical Phase-Shifting Transformer model

In open literature [13, 14] it is common to represent the phase-shifting transformer as an impedance connected in series with an ideal transformer having a complex turns ratio. Figure 2 shows the equivalent circuit of the PST connected between nodes p and s . The transformer phase shifting capabilities are taken to be on node p .

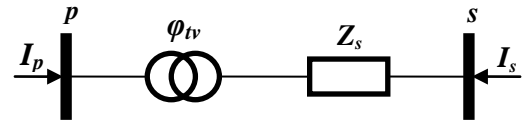


Figure 2: Equivalent circuit to PST.

The classical PST model can be obtained by introducing simplifying assumptions in the two-winding transformer model given in [2]. If $T_v = T_i^* = \cos\phi_{tv} + j\sin\phi_{tv} = a + jb$, $U_v = U_i^* = 1$, $Y_o = 0$ and $Z_p = 0$, a nodal transfer admittance model for the PST shown in Figure 2 can be obtained,

$$\begin{bmatrix} I_p \\ I_s \end{bmatrix} = \frac{1}{(a^2 + b^2)Z_s} \begin{bmatrix} 1 & -(a + jb) \\ -(a - jb) & (a^2 + b^2) \end{bmatrix} \begin{bmatrix} V_p \\ V_s \end{bmatrix} \quad (5)$$

3) Power flow equations

Based on the nodal admittance matrix equation given by (5), the following active and reactive power equations can be written for a two-winding transformer connected between node p and node s [2].

At node p :

$$P_{p_inv_{PST}} = V_p^2 G_{pp} + V_p V_s (G_{ps} \cos(\theta_p - \theta_s) + B_{ps} \sin(\theta_p - \theta_s)) \quad (6)$$

$$Q_{p_inv_{PST}} = -V_p^2 B_{pp} + V_p V_s (G_{ps} \sin(\theta_p - \theta_s) - B_{ps} \cos(\theta_p - \theta_s)) \quad (7)$$

At node s :

$$P_{s_inv_{PST}} = V_s^2 G_{ss} + V_s V_p (G_{sp} \cos(\theta_s - \theta_p) + B_{sp} \sin(\theta_s - \theta_p)) \quad (8)$$

$$Q_{s_inv_{PST}} = -V_s^2 B_{ss} + V_s V_p (G_{sp} \sin(\theta_s - \theta_p) - B_{sp} \cos(\theta_s - \theta_p)) \quad (9)$$

where P_p , P_s , Q_p , Q_s are the active and reactive power flow injections at nodes p and s . V_p , V_s , θ_p , θ_s are the voltage magnitudes and phase angles at nodes p and s , respectively. It must be mentioned that the susceptance and conductance are dependents of ϕ_{tv} .

The PST can have various applications in power systems, however, in this work is used to control the active power flow at a desired level in the compensated branch ($i-j$). The active power flow, P_{ij} , through branch $i-j$ is controlled in P_{esp} value by the PST connected between nodes i and j . This control action can be represented by next control equation,

$$P_{ij} - P_{exp} = 0 \quad (10)$$

where $i=s, p; j=s, p; i \neq j$ and P_{ij} is the active power injected by the PST device (P_{i_injPST}) in the compensated transmission line, which is a function dependent of control variable ϕ_{lv} .

IV. PST-OPF EXPLICIT MODELING

The conventional OPF explicit modelling given in [11] is adopted and extended to readily develop the PST-OPF formulation by considering the PST model shown in Section III-B. The OPF general model (1)-(4) is the basis to derive the explicit PST-OPF model, as will be explained below.

A. Objective function

The objective function $f(y)$ is the minimization of the total active power generation costs,

$$f(y) = \sum_{i=1}^{N_g} a_i + b_i (P_{gi}) + c_i (P_{gi})^2 \quad (11)$$

where a_i, b_i and c_i are the cost curve coefficients for the generation bus i . N_g is the number of generators, whose individual active output power is P_{gi} .

B. Equality constrains

In order to represent the system steady state operation, the energy balance of the power system must be unconditionally satisfied. This is enforced by means of the set of active and reactive power balance constraints at each bus,

$$h(y) = \left\{ \begin{array}{l} P_{gi} - P_{li} - \sum_{j \in i} P_{inj} - \sum_{j \in i} P_{j_injPST} = 0, \\ Q_{gk} - Q_{lk} - \sum_{j \in k} Q_{inj} - \sum_{j \in k} Q_{j_injPST} = 0 \end{array} \right\} \quad i=1,2,\dots,N_b \quad k=1,2,\dots,N_b, k \neq N_g \quad (12)$$

where N_b is the total number of buses. The active and reactive output power of generator P_{gi} and Q_{gi} , respectively, are provided at the generation bus $j(j=i,k)$. The active and reactive power loads are represented by P_{lj} and Q_{lj} , respectively. $\sum_{j \in i,k}$ is the set of nodes adjacent to node j , whilst P_{inj} and Q_{inj} are active and reactive power flows injected at bus k and i through the j -esim network element described by models of Section III. Note that the power balance constraints (12) must consider the injected power P_{j_injPST} and Q_{j_injPST} provided by each PST controller, according to models given by (6)-(9). Clearly, the incorporation of each PST controller into the conventional OPF model implies the introduction of one new state variable, which corresponds to phase shifter angle ϕ_{lv} . In addition, the power flow control equation (10) of the PST must be considered as an additional equality constraint, which is given by (13),

$$h_{ctrl}(y) = \{P_{ij,n} - P_{exp,n} = 0\}, n=1,2,\dots,N_{PST} \quad (13)$$

where N_{PST} is the number of PST controller operating in the power network. P_{ij} is the active power flowing from node i to node $j, i=l,m, j=l,m, i \neq j$. $P_{sh,n}$ is the target value of active power flow across the n -esim PST device.

In the optimization formulation, the constraints (13) represent the active power flow control action of the PST controllers. Hence, these control actions are expressed as equality constraints which remain active throughout the whole iterative optimization

process. If the active power flow control of the PST is at off state, constraint (13) is deactivated. The equations (12)-(13) represent the full set of equality constraints of the PST-OPF formulation.

It is very important to point out that the generator reactive output power Q_{gi} is a function of the system variables and does not have a scheduled value, therefore the reactive power balance constraint can be only stated for non-generation buses ($k \notin N_g$). However, the reactive power balance at generation buses is achieved according to the procedure applied to handle the reactive generation limits, as will be explained in the next section.

C. Inequality constrains

The physical and operating limits of generators and substations are mathematically described by the following inequality sets,

$$Y = \left\{ \begin{array}{l} P_{gi}^{\min} \leq P_{gi} \leq P_{gi}^{\max} \\ V_j^{\min} \leq V_j \leq V_j^{\max} \end{array} \right\}, i=1,2,\dots,N_g, j=1,2,\dots,N_b \quad (14)$$

$$g(y) = \{Q_{gi}^{\min} \leq Q_{gi} \leq Q_{gi}^{\max}\}, i=1,2,\dots,N_g \quad (15)$$

It must be pointed out that the active power generation P_{gi} and all the bus magnitude V_j limits are simply inequality constraints on variables, whilst the generator reactive power limits are modeled as a set of functional inequality constraints. Hence, the reactive power generation level Q_{gi} in (15), is given by the following function,

$$Q_{gi} = Q_{li} + \sum_{j \in i} -V_i^2 B_{ij} + V_i V_j [G_{ij} \sin(\theta_i - \theta_j) - B_{ij} \cos(\theta_i - \theta_j)] \quad (16)$$

The relation (16) means that the reactive power balance generation bus i is always achieved when the generator is inside its reactive generation limits. When the generator hits either its lower Q_{gi}^{\min} or upper Q_{gi}^{\max} bound, the inequality constraint (15) is activated by the optimization algorithm, it then automatically becomes into an equality constraint in order to enforce the reactive power generation level Q_{gi} to be the violated limit Q_{gi}^v ,

$$Q_{gi}^v - Q_{gi} = 0 \quad (17)$$

where Q_{gi} is defined by (16). Note that constraint (17) not only avoids the violation of the reactive power generation limits, but also represents the reactive power balance equation.

In the PST-OPF formulation, the state variable limits, ϕ_{lv} , of each PST controller must be included as an inequality constraints set, as follows,

$$Y_{PST} = \{\phi_{lv,i}^{\min} \leq \phi_{lv,i} \leq \phi_{lv,i}^{\max}\}, i=1,2,\dots,N_{PST} \quad (18)$$

The corresponding lower ϕ_{lv}^{\min} and upper ϕ_{lv}^{\max} limits are simply represented by inequality constraints on variables. These limits allow simulating more practical operating conditions of the PST controller.

V. PST-OPF PRACTICAL IMPLEMENTATION

The PST-OPF explicit model (11)-(18) has been developed by implementing the PST model into an existent computational algorithm for conventional OPF [11], which is solved by means of the Matlab optimization toolbox [10].

From an optimization point of view, the PST-OPF model represents a continuous nonlinear constrained optimization problem, which can be also solved by using the *fmincon* function

of Matlab optimization toolbox [10]. This function uses a Sequential Quadratic Programming optimization algorithm, started with input/output arguments to configure the optimization parameters, set the model to be optimized and display information.

A. Arguments of the *fmincon* function

The *fmincon* function, as any Matlab function, deals with both input I_A and output O_A arguments. The general form of this function is [10],

$$[O_A]=fmincon(I_A) \tag{19}$$

where I_A and O_A are sets of input and output arguments, respectively. Tables I and II briefly show and describe the main elements of these argument sets according to the order they must be provided to the *fmincon* function. Details of the option parameters $Opt \in I_A$ and output $\in O_A$ are given in [10].

TABLE I: Description of the input arguments I_A .

Name	Description
@fun	The handle of the M-function file containing the objective function, in our case; @(X)objfun_OPF(X).
X	The vector containing the numerical value of the initial condition of system and PST variables ($\theta, V, P_g, \phi_{iv}$).
A	All these parameter are not of interest in this work, they refer to linear equality and inequality constraints. They simply are set as empty arguments ([]).
B	
Aeq	
Beq	
Lb	Vector of lower bounds value of variables, in this work applied to the sets V, P_g and ϕ_{iv} .
Up	Vector of upper bounds value of variables, in this work applied to the sets V, P_g and ϕ_{iv} .
Nlcon	The handle of the M-function file containing the nonlinear equality and inequality functional constraints, here; @(X)constraints_OPF(X).
Opt	This structure provides optional parameters for the optimization process, which are set by means the optimset function of Matlab.

TABLE II: Description of the output arguments O_A .

Name	Description
X	This vector contains the numeric value of the system variables at the PST-OPF model solution, and is the same vector considered in I_A (see Table I).
fval	Value of the objective function at the solution X.
eflag	Describes the exit condition of <i>fmincon</i> ; if eflag>0, the convergence was reached. If eflag=0, the maximum number of iteration was exceeded. If eflag <0, there was not
output	Structure that contains information of the optimization process results.
λ	Vector of Lagrangian multipliers at the solution X.
Grad	Value of the Gradient of the objective function at the solution X.
Hess	Value of the Hessian of the objective function at the solution X.

B. PST-OPF computational implementation

In order to implement a general PST-OPF program for digital computer, the PST-OPF model is solved by using the *fmincon* function, which is executed according to the computational procedure described in Figure 3. The proposed PST-OPF

computational implementation starts reading the power system data and convergence tolerance. The power system data are converted to pu in order to normalize the system quantities, but also to avoid optimization scaling problems. The system variables are initialized as follows, nodal voltage magnitudes V are set to 1 pu and angles θ are set to 0 rad, as in conventional power flow analysis. The active power generation levels P_g are initialized according to a network lossless Economic Dispatch (ED) analysis. In case of the PST variables, the primary and secondary complex taps are set with a magnitude of one and phase angle of zero, i.e. the phase shifter angles are initialized at 0° , although the algorithm of this proposed is very robust if the phase shifter angle is initialized within the range of $\pm 10^\circ$.

This analysis is formulated as a nonlinear programming problem, where the objective function (11) is the considered in the PST-OPF model; the equality constraint are the active power balance between the total generation and the total load in each bus of the power system, whilst the inequality constraints only correspond with the generation active power limits. The constraints and the objective function are written in two separated Matlab functions M1 and M2, respectively, which are called by the *fmincon* function executed from the implemented ED function.

The vector of initial conditions X is then passed to the implemented PST-OPF function, where the *fmincon* function is newly executed to obtain the solution of the PST-OPF model. The constraints (12)-(18), are written in another Matlab function (M3), called by *fmincon*, along with the objective function (11) written in M2, from the implemented PST-OPF function. The optimal solution X is used to compute the network active and reactive power flows, which are finally reported in a text file and on the computer display.

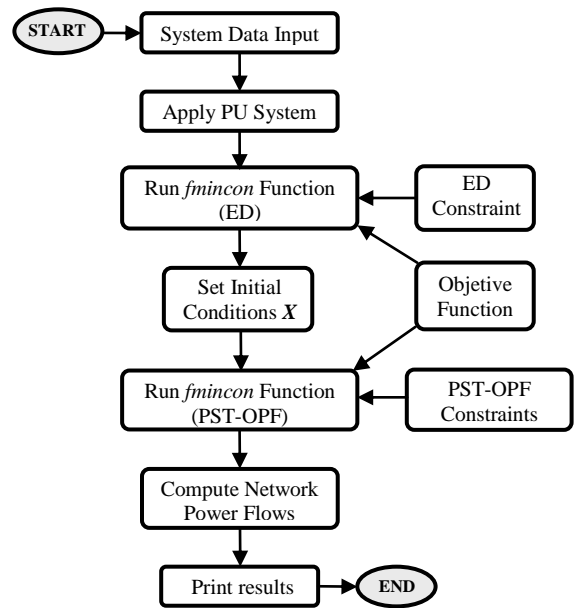


Figure 3: PST-OPF computational algorithm.

VI. NUMERICAL EXAMPLES

In order to illustrate numerically the prowess of the proposed implementation to carry out the PST-OPF analysis, the IEEE 5-node system and the 10-machine 39-bus New England system are considered in the numerical examples. In both test cases, the convergence tolerance of the optimization process is set at 1×10^{-9} and the phase shifting angle was initialized at 0° .

A. Test case: 5-node system

This section presents the PST-OPF results for the 5-node test system obtained by the proposed implementation. The aim of this case study is to numerically compare results of the proposed approach with those reported in [2]. In order to embed the PST, the test system was enlarged by adding the node Lake1 to the network, as in [2]. The PST is used to maintain the active power flow at 25 MW across the transmission line Lake-Main. In this test case, the primary and secondary winding impedances contain no resistance. The primary and secondary inductive reactances were set to 0.0 pu and 0.05 pu, respectively. The complex tap ratios were $T_v = U_v = 1.0 \angle 0^\circ$. The control of active power flow is carried out with the primary phase angle control. The nodal voltages are initialized with flat profile; the voltage magnitude limits for all nodes are set to $0.9 \leq V \leq 1.1$ pu, except at node North, where the voltage magnitude limit is set to $0.9 \leq V \leq 1.5$ pu.

The results of the optimal active and reactive power dispatches are displayed in Table III, both dispatches obey their corresponding limits.

Table III: Generators ratings and PST-OPF solution.

Node	MW Limits		MVAR Limits		OPF Dispatch	
	Lower	Upper	Lower	Upper	MW	MVAR
North	10	400	-500	500	79.81	1.22
South	10	400	-300	300	88.48	14.47
Total Power Generation					168.29	15.69

The Table IV shows that the profile of nodal voltages is inside limits. However, it must be pointed out that because of the voltage magnitude at node South hits its upper limits, the corresponding inequality constraint is activated and therefore it has a value equal to the upper limit.

Table IV: Nodal voltages at the PST-OPF solution.

Node	V (pu) Limits		OPF Voltages	
	Lower	Upper	V (pu)	θ (deg)
North	0.9	1.5	1.11	0.000
South	0.9	1.1	1.10	-1.461
Elm	0.9	1.1	1.07	-4.892
Main	0.9	1.1	1.08	-4.963
Lake	0.9	1.1	1.08	-2.895
Lake1	0.9	1.1	1.076	-4.580

The solution obtained by the proposed implementation compares well with that reported in [2], as illustrated in Table V. The solution was obtained in a CPU time of 5.1792 sec with a total generation cost of 748.961 \$/hr and total losses of active power of 3.285 MW. The table shows that the solutions are very similar, therefore it can be concluded that the proposed implementation is reliable for the analysis of OPF model with the PST device.

Table V: Comparison of two different solutions of PST-OPF model.

Parameter	Proposed	[2]
Cost (\$/hr)	748.961	748.330
Losses (MW)	3.285	3.143
Control angle (deg)	-1.0026	-2.010
Active power generation (MW)	168.29	168.13
Reactive power generation (MVAR)	15.69	15.25

B. Test case: 10-machine, 39 bus New England system

In this section the proposed implementation is used to carry out the PST-OPF analysis on the 10-machine 39-bus New England system shown in Figure 4. The parameters of the system are given in detail in [15] and the generators cost functions and ratings are given in [16]. The voltages magnitude limits for all nodes are set to $0.95 \leq V \leq 1.09$ pu.

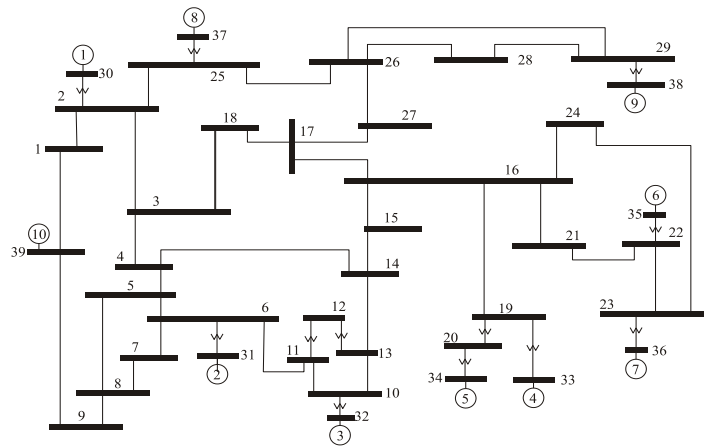


Figure 4: 10-machine, 39 bus New England test system

Firstly, a conventional OPF analysis (base case) is executed. This base case computes an optimal steady state operating point with a total generation cost of 61,214.142 \$/hr, and reveals that 264.71 MW are transferred from node 26 to 27 across the single line connecting both nodes. Then, at node 27, the load increases from 281 MW to 300 MW, changing the power flow in all lines connected to the node and the New England system is modified to integrate the PST device to the power system. A new node, 40-PST, was added to include the PST controller in the power system, which is strategically connected in the electric power system to increase the active power flow from 264.71 MW to 266.5 MW in the transmission line connected between nodes 26 and 27. The PST device parameters were the same as in the above test case. The Table VI summarizes the results of the conventional OPF (base case) and the PST-OPF analysis.

Table VI. Summary results of PST-OPF and OPF.

Results	OPF (Base Case)	PST-OPF
MW flow in compensated line	264.71	266.50
Generation (MW)	6,158.28	6,157.73
Generation (MVAR)	1,213.72	1,245.55
Losses (MW)	42.181	41.625
Cost (\$/hr)	61,214.142	61,213.142

To carry out the control action of the active power flow in MW 266.5 across the compensated transmission line connected between node 26 and 27, the phase shifting angle, φ_{ns} , changed his value from 0° to -7.3145° .

The CPU time required to carry out the PST-OPF solution with the New England system was of 34.4531 sec. It is noteworthy that the numerical examples were executed in an Asus PC with Intel(R) Core(TM) i5-3210M processor at 2.5 GHz and 6 GB of RAM.

VII. CONCLUSIONS

The proposed PST-OPF model is written into a unified reference frame, such that the whole set of electrical variables (voltage phasors and powers) and variables of PST-OPF can be solved simultaneously. But it must be pointed out that the proposed formulation readily allows to either consider or not the steady state operation of a given FACTS device into the power system simulation. The PST-OPF model was integrated into an OPF Matlab-based model, and the solution process uses the *fmincon* function of the Optimization Toolbox. Independently of the value of the initial condition of the state variables, the PST model presents very good robustness towards convergence and yields practical solutions. Solutions have been obtained through numerical examples where the OPF problem is integrated with FACTS devices. The results show that the proposed implementation allows simulating the economic operation of power systems readily. The time required to compute the optimal steady state is short enough for academic and/or research purposes, and perhaps promising to carry out power system planning studies.

Another advantage of this proposal is that the PST model is easily implemented into the OPF formulation due to the flexibility provided by the optimization toolbox of Matlab. Taking advantage of this easiness, the model of any other device of the FACTS family, as well as a large variety of optimization applications of power systems, can be readily integrated into the conventional OPF model.

ACKNOWLEDGMENT

Financial support given by Instituto Tecnológico Superior de Irapuato to develop this work is gratefully acknowledged.

REFERENCES

- [1] Kappenman J.: 'Static Phase Shifter Applications and Concepts for the Minnesota-Ontario Interconnection', Flexible AC Transmission Systems (FACTS) Conference, EPRI, Boston Massachusetts, 18-20 May, 1992.
- [2] Ambriz-Pérez H. "Flexible AC Transmission Systems Modelling in Optimal Power Flows Using Newton's Method", Ph.D. Thesis, Department of Electronics and Electrical Engineering, University of Glasgow, UK, December 1998.
- [3] KNITRO. [Online]. Available: <http://www.ziena.com>.
- [4] A. S. Drud, *GAMS/CONOPT*, ARKI Consulting and Development, Bagsvaerdvej 246A, DK-2880 Bagsvaerd, Denmark, 1996, available at <http://www.gams.com/>.
- [5] W. Rosehart, C. Roman, and Antony Schellenberg, "Optimal Power Flow with Complementary Constraints". *IEEE Trans. Power Syst.*, Vol. 20, No. 2, pp. 813-822, May 2005.

- [6] R. J. Avalos, C.A. Cañizares, F. Milano, and A. J. Conejo, "Equivalency of Continuation and Optimization Methods to Determine Saddle-Node and Limit-Induced Bifurcations in Power Systems". *IEEE Trans. on Circuits and Systems*, Vol. 56, No. 1, pp. 210-223, January 2009.
- [7] R. Zárate-Miñano, T. Van Cutsem, F. Milano and A. J. Conejo, "Securing transient stability using time-domain simulations within an optimal power flow". *IEEE Trans. on Power Syst.*, vol.25, no.1, pp. 243-253, Feb. 2010.
- [8] V.J. Gutierrez-Martinez, C.A. Cañizares, C.R. Fuerte-Esquivel, A. Pizano-Martínez, and X. Gu, "Neural-network security-boundary constrained optimal power flow". *Transactions on Power Systems*, 2010.
- [9] A. Lashkar Ara, A. Kazemi and S. A. Nabavi Niaki, "Multiobjective Optimal Location of FACTS Shunt-Series Controllers for Power System Operation Planning", *IEEE Transactions on Power Delivery*, Vol. 27, No. 2, pp. 481-490, April 2012.
- [10] The MathWorks, Inc., "Matlab Optimization Toolbox," Users Guide Version 2, available at <http://www.mathworks.com>.
- [11] Pizano-Martínez, A., Fuerte-Esquivel, C., Zamora-Cárdenas, E.A., and Segundo Ramírez, J., "Conventional Optimal Power Flow Analysis Using the Matlab Optimization Toolbox," ROPEC International 2010.
- [12] Acha E., Fuerte Esquivel C. R., Ambriz Pérez H. and Angeles Camacho C.: *FACTS: Modelling and Simulation in Power Networks*. John Wiley and Sons, 2004.
- [13] Peterson N.M. and Scott-Meyer W.: 'Automatic Adjustment of Transformer and Phase Shifter Taps in the Newton Power Flow', *IEEE Transactions on Power Apparatus and Systems*, Vol. PAS-90, No. 1, January/February 1971, pp. 103- 108.
- [14] Shen C.M. and Laughton M.: 'Determination of Optimum Power-System Operating Conditions Under Constraints', *Proceedings of IEE*, Vol. 116, No. 2, February 1969, pp. 225-239.
- [15] M. A. Pai, *Energy Function Analysis for Power System Stability*. Kluwer, 1989.
- [16] T. B. Nguyen and M. A. Pai, "Dynamic security-constrained rescheduling of power systems using trajectory sensitivities," *IEEE Trans. Power Syst.*, vol. 18, no. 2, pp. 848-854, May 2003.

AUTHORS

First Author – José Miguel García Guzmán, M. Sc. Electrical Engineering, Department of Electromechanical Engineering, Instituto Tecnológico Superior de Irapuato, migarcia@itesi.edu.mx.

Second Author – Francisco Javier Ortega Herrera, M. Sc. Mechanical Engineering, Department of Electromechanical Engineering, Instituto Tecnológico Superior de Irapuato, frortega@itesi.edu.mx.

Third Author – Jacinto Torres Jiménez, PhD. Electrical Engineering, Department of Posgraduate in Electrical Engineering, Instituto Tecnológico Superior de Irapuato, jacinto.torres@itesi.edu.mx.

Fourth Author – Guillermo Tapia Tinoco, M. Sc. Electrical Engineering, Department of Posgraduate in Electrical Engineering, Instituto Tecnológico Superior de Irapuato, gutinoco@itesi.edu.mx.

Fifth Author – Luis Alberto Contreras Aguilar, PhD. Electrical Engineering, Department of Posgraduate in Electrical Engineering, Instituto Tecnológico Superior de Irapuato, lucontreras@itesi.edu.mx.

Correspondence Author – José Miguel García Guzmán, migarcia@itesi.edu.mx, terrysa83@hotmail.com, Tel: 01 462 606 7900, Ext. 130.